Journal of Polymers and the Environment (2024) 32:1217–1232
https://doi.org/10.1007/s10924-023-03019-1

RESEARCH

Poly(Ethylene-*Co*-Vinyl Acetate)–Poly(Lactic Acid)–Poly(Styrene-*Co*-Methyl Methacrylate) Blends: Study of Mechanical Properties Under Hydrolytic Degradation and Cytotoxic Evaluation

Mónica Elvira Mendoza-Duarte[1,2] · Jorge Alberto Roacho-Pérez[3] · Adriana G. Quiroz- Reyes[3] · Elsa N. Garza-Treviño[3] · Celia N. Sánchez-Domínguez[3] · Perla Elvia García-Casillas[4] · Alejandro Vega-Rios[1]

Accepted: 3 August 2023 / Published online: 31 August 2023

Abstract

The present research investigates the hydrolytic degradation of ternary blends composed of poly(ethylene-*co*-vinylacetate) (EVA), poly(lactic acid) (PLA), and poly(styrene-*co*-methyl methacrylate)(poly(S-*co*-MMA) (SMMA) (EPS) blends at a temperature of 37 °C and pH 7.4, monitoring the changes in phosphate buffer solution for 6 months. In addition, the mechanical behavior and morphology of the blends were evaluated from the comparison with the degraded blends against probes non-hydrolytically degraded. Likewise, the hemolytic properties and the cytotoxicity of the blends were estimated to determine their safety if used in medical devices. Ternary blends with higher stiff-elongated properties were composed of 30 wt% EVA—69 wt% PLA and 1 wt% SMMA and prepared by varying the mixing time of each component. EPS samples presented less hydrolytic degradation than PLA. Blending PLA with EVA and SMMA resulted in significant mechanical stability throughout the degradation time. Biocompatibility tests reported that the interaction of EVA/PLA/SMMA films with mesenchymal stem cells showed no evidence of damage in the metabolism of the cells; thus, the films were not dangerous. Furthermore, all tested samples reported values below 5% of hemolysis; hence are classified as non and slightly hemolytic according to ASTM F756. Therefore, polymer EPS blends have potential applications in medical devices.

Graphical abstract

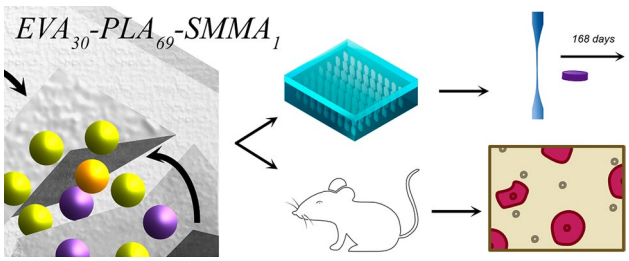

Keywords PLA · EVA · SMMA · Blends · Mechanical properties · Hydrolytic degradation · Cytotoxicity · Hemolysis

Introduction

A biomaterial used as a medical device must have intrinsic characteristics that allow its application with a long-term duration and without rejection by the human body [1, 2]. Among the polymeric biomaterials that have been investigated for biomedical devices is poly (lactic acid) (PLA) [3]. PLA is an aliphatic bio-based polymer, preferable in biomedical applications due to its biocompatibility, biodegradability, and low toxicity [4]. PLA is used in a wide range of biomedical applications, such as stents [5–7], surgical sutures [8, 9], and screws [10], among others. However, the general criterion for selecting a

Extended author information available on the last page of the article

polymer for its use in a medical application is to balance the mechanical properties and the required degradation time. Therefore, the selection requires an in-depth characterization of the changes in strength and stiffness of the polymeric material during degradation [7], to maintain mechanical stability during this stage. Understanding the PLA properties is the key to achieving suitable chemical and biological properties.

The degradation behavior of PLA is a vital feature and a significant reason for its use in medical applications [7]. However, it presents some limitations, such as hydrophobicity and inadequate mechanical properties for bone repair [11, 12]. Amorphous PLA polymer has low tensile strength, higher elongation at break, and more rapid degradation time than semicrystalline PLA, making it more attractive as a drug delivery system [7, 13]. Specifically, in orthopedic and fixation devices, an advantage of a PLA medical device is that it does not have to be removed, avoiding a second surgery and reducing costs because it degrades simply by hydrolysis without using enzymes or catalysts [7, 14–16].

Although the biodegradability of materials used in the manufacture of medical devices is desirable, the polymer degradation rate must be customized to be safe without cytotoxic or inflammatory reactions [17–19]. Velioglu et al. [20] evaluated the potential of utilizing PLA in medical devices. They studied the attachment and proliferation of human bone marrow mesenchymal stem cells of 3D-printed poly(lactic acid) scaffolds concluding that PLA scaffolds appear as an alternative for bone repair and regeneration. The key to medical device success is to balance the presence of additives, the geometry of the device, and its location to adapt an implant for slow degradation and transfer stress to the surrounding tissue as it heals at the appropriate rate. Another requirement for materials intended for contact with blood, e.g., medical devices, is to evaluate their hemolytic properties. The presence of hemolytic material may produce increased levels of free plasma hemoglobin capable of inducing toxic effects or other consequences which may stress the kidneys or other organs [21].

On the other hand, some authors have studied the hydrolytic degradation of PLA in PBS solution at 37 °C [22, 23] and under different temperatures. For example, Gorrasi and Pantani [24] reported the hydrolysis process during 60 days of PLA with different D-isomer content by immersion in distilled water at 58 °C and a pH of 5.7. The degradation medium was replaced every day. Around day 30, they found that PLA 4060D (PLA with the highest D enantiomer content) showed the fastest rate of weight loss with a value of 70%. Likewise, Wei et al. [25] investigated the hydrolytic degradation behavior of PLLA grafted with poly(β-myrcene) (PM) rubber during 90 days, registering a mass loss of the PLLA homopolymer around 73.9%, while the PM-g-PLLA copolymers registered less than 5%.

Nevertheless, PLA exhibits fragile behavior and low elongation [26–28]. The polymer blend is an efficient and cost-effective method for tailoring and modifying properties [29]. In particular, PLA generates a new degradation profile that depends on the type of polymer added, the relationship, and the morphology of the blend [8]. In addition, PLA can be blended with other polymeric components to cover most required properties in worldwide application requirements [17]. Furthermore, two significant challenges to stabilizing PLA are its water permeability and autocatalytic reaction [17]. Therefore, melt blending is ideal for modifying polymer properties and does not employ any solvent-avoiding non-desirable residual solvent toxic effects, which medical devices require [30]. In addition, minimal attention has been given to studying blend stability under different hydrolytic degradation conditions [7].

Moreover, Liu et al. [31] investigated the in vitro degradation behavior of PLLA/aragonite and PLLA/vaterite blends. They observed that blending the PLLA can decrease its rate of hydrolysis. Navarro et al. [32] studied in vitro biodegradation of PLA/PCL blends at 37 °C for 140 days in a PBS solution replaced once a week. They found that under the conditions established in vitro test, PLA degrades by chain scission of polymer chains with a decrease of molecular weight but without weight loss. Wongwiwattana and Thomas [33] conducted degradation tests in PBS solution for 260 days at 37 °C of PLA/PCL, indicating that PLA undergoes bulk degradation.

The obtention of PLA/EVA and PLA/SMMA binary blends has been previously investigated separately [30, 34–39]. In particular, PLA/EVA blends have already been considered for medical applications [30, 37, 40]. There are few reports about PLA/PMMA blends as an option for medical applications [41].

In the previous study, we investigated the effect of mixing PLA with EVA and SMMA (EPS) obtained by melt blending to improve its mechanical behavior regarding elongation at break and stiffness [34]. The addition of EVA improved the elongation at break of PLA, while SMMA contributed to preserving the stiffness. In addition, the effect of processing and incorporation times of the components in the mechanical properties was studied [34]. In contrast, in this research, we explore these polymer blends with potential applications in medical devices. This study aimed to determine the mechanical properties and morphology of the EPS blends during hydrolytic degradation, specifically in phosphate buffer solution (pH 7.4) at 37 °C. Furthermore, the cytotoxicity and hemolytic effect of these blends were evaluated for their application in medical devices.

Materials and Methods

This research work was authorized by the Ethics Committee of the Universidad Autónoma de Nuevo León, School of Medicine with registration number BI19-00003 and Dr. José Eleuterio González University Hospital of the Universidad Autónoma de Nuevo León. All animals and human donors were treated according to ethical standards.

Materials

Poly (L,D-lactide) PLA Ingeo 4060D, (8%–10%) D [42], from NatureWorks LLC, USA, with an average molecular weight Mw—190 kg/mol, $\rho = 1.24$ g/cm^3 and glass transition temperature $T_g = (55–60)$ °C.

Poly(ethylene-*co*-vinyl acetate) (EVA), commercial name EVA 2810-A ATEVA CELANESE with 28% vinyl acetate, $\rho = 0.949$ g/cm^3, $T_m = 73$ °C, MFI = 6. Poly(styrene-*co*-methyl methacrylate) Poly(S-*co*-MMA), SMMA NAS®30, $\rho = 1.090$ g/cm^3, $T_g = 103$ °C, MFI = 2.2, from Ingeos Styrolution Group GmbH, Germany with the content of styrene (70–90%) and methyl methacrylate (10–30%). Phosphate salt (PBS) capsules from Sigma-Aldrich, bone marrow mesenchymal stem cells (BM-MSC) were obtained from BALB/c mice. CO_2 gas, DMEM/nutrient mixture, FBS, gentamicin, and amphotericin (Gibco; Thermo Fischer Scientific, Waltham). Cell culture flasks (Corning, Inc.). MMT Solution (Cell proliferation Kit I, Roche, Basilea Switzerland). Isopropanol, methanol, HCl (Sigma Aldrich), and BD Vacutainer® heparin tubes (Becton Dickinson).

Table 1 Formulations of polymer blends produced

Sample	EVA content (%)	PLA content (%)	SMMA content (%)	Mixing time (min)
PLA5	–	100	–	5
PLA15	–	100	–	15
EPS1	30	69	1	5
EPS2	30	69	1	15
EPS3	30	69	1	15, 5*

*First, PLA was mixed with EVA for 15 min, and then SMMA was added for 5 min before completing 15 min of mixing

Melt Blending

The ternary polymer blends EVA/PLA/SMMA (EPS) were prepared following the procedure reported in our previous paper [34]. The formulations chosen for the present study are summarized in Table 1. The ternary polymer blends EVA/PLA/SMMA (EPS) were prepared in a Brabender internal mixer (BB) [DDRV501, C.W. Brabender Instruments Inc., Hackensack, NJ, USA] at a temperature of 180 °C, see Fig. 1a. Table 1 shows the formulations of manufactured polymer mixtures. To remove moisture that polymers might contain and prevent possible hydrolysis degradation during processing, the pellets were dried previously at 60 °C for 12 h employing an Isotemp model 281 vacuum oven.

Films and Probes Elaboration

The blends obtained were cooled to room temperature and ground using a blade mill, Fritsch model Pulverisette. To determine the mechanical properties and to evaluate the cytotoxicity of the blends, thin films (thickness of 0.15 mm) and type V probes (ASTM D638) [43] were compression molded using a hydraulic compression molding press (Carver Inc. Wabash, IN, USA) at a temperature of 180 °C, the applied force was 5 metric Ton, see Fig. 1b.

Hydrolytic Degradation

The experiments were conducted in phosphate-buffered saline solution (PBS) (pH = 7.4 ± 0.1, Fisher Scientific) at a temperature of 37.0 ± 0.1 °C, see Fig. 1c. Twenty-one probes (ASTM D638 Type V) of each formulation (EPS1, EPS2, EPS3, PLA5, and PLA15) were placed vertically inside

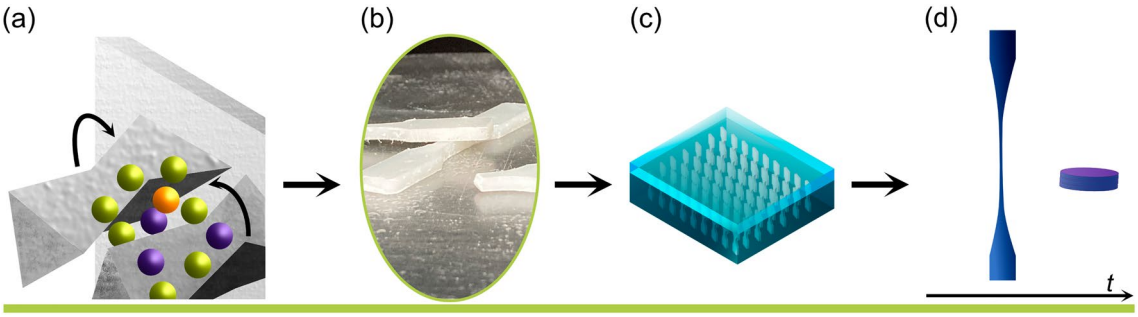

Fig. 1 Experimental design. **a** Blends preparation, **b** obtention of probes and films, **c** array of probes for hydrolytic degradation at 37 °C in PBS, and **d** characterization at different degradation times

acrylic boxes, and a PBS solution (2 L) was added, covering 1 cm above the sample. In addition, three specimens of each formulation were removed from the boxes at 1, 7, 21, 35, 42, 84, and 168 days for evaluation. The probes were incubated in a forced air oven at 37.0 °C until 168 days. The PBS solution was not changed during the experiment, and a box was utilized for each sample, see Fig. 1c.

Obtention of an MSC Primary Culture

Bone marrow mesenchymal stem cells (BM-MSC) were obtained from BALB/c mice. In addition, three mouses were placed inside a CO_2 chamber (70% vol/min) to sacrifice them. Immediately after, their femurs and tibias were dissected under aseptic conditions. Epiphysis was removed, so BM was obtained using a hypodermic needle (27 gauge) by perfusing the shafts inner barrel with 500–1000 µL DMEM/Nutrient Mixture F-12 (DMEM F-12) medium supplemented with 10% FBS, 100 µg gentamicin/mL, and 2.5 µg amphotericin B/mL (Gibco; Thermo Fisher Scientific, Waltham, MA, USA), and poured into T-25 cell culture flasks (Corning, Inc.). Cells were incubated for 24 h at 37 °C in a 5% CO_2 humid atmosphere. The culture flasks with the adherent cells were replenished with 4 mL of fresh supplemented DMEM F-12 medium and incubated before the cell monolayer reached 80% confluence (7–10 days). The expended medium and the non-adherent cells were discarded.

Characterization

Water Absorption and Remaining Mass

The initial weight (W_i) of the samples was registered prior to hydrolytic degradation using a 4-digit analytical balance (OHAUS Adventurer AR3130). Subsequently, the weight of three samples at a specific time (1, 7, 21, 49, 84, and 168 days) was registered. Then, samples were weighed to determine their wet weight (W_w) by removing excess water with Kimwipes (Kimtech science, Kimberly-Clark). Later, these probes were rinsed with distilled water and dried at 25 °C for 72 h at a set vacuum of 0.8 bar until constant dry weight (W_d). Finally, the percentage of water absorption ($W_{absoprtion}$) and the remaining mass (R_{mass}) were determined according to Eq. (1) [31] and Eq. (2) [44], respectively.

$$W_{absorption}(wt\%) = \left(\frac{(W_w - W_d)}{W_d}\right) \times 100 \quad (1)$$

$$R_{mass}(wt\%) = \left(\frac{W_d}{W_i}\right) \times 100 \quad (2)$$

pH

The pH value of the PBS solution was measured using a pH meter (Thermosicentific Eutech Elite pH, Singapore) at the previously designated periods.

Mechanical Evaluation

The mechanical properties were tested utilizing a Universal Instron testing machine at room temperature following the Standard Test Method for Tensile Properties of Plastics, ASTM D638, see Fig. 1d. The samples were subjected to uniaxial tension at a constant displacement rate of 1 mm/min until the break. Three samples were analyzed for each blend or PLA; the result is the average of these measurements.

Scanning Electron Microscopy

Surface and cross-section morphology of the PLA and its blends were observed employing a scanning electron microscope, Hitachi SU3500, operated at 5.00 kV. Cross-section samples were prepared by cryo-fracture of the probes by immersion in liquid nitrogen. The samples were coated with a thin layer of gold prior to analysis.

Cytotoxicity: MTT Assay

In order to evalute the possible damage that EPS1, EPS2, and EPS3 can cause to cells, decreasing in vitro cell viability, an MTT assay was performed according to ISO-10993-5. A total of 10,000 MSC were seeded per well in a 96 well microplate. Cells were cultured at 37 °C in a CO_2 atmosphere (5%) with supplemented DMEM F-12 medium. Following 72 h of culture, cells were exposed to PLA 5, PLA 15, EPS1, EPS2, and EPS3 by quadruple. Samples were cut in circular shapes with 6 mm diameter. Cells with no film exposure were taken as a negative control. The samples were previously sterilized for 15 min using UV light exposition on each side. After 24 h of exposition with the films, cell death was measured by MTT assay. Media were removed, and cells were incubated with 100 µL of the MTT solution (Cell Proliferation Kit I, Roche, Basilea, Switzerland) for 3 h. After incubation, 100 µL of isopropanol pH 3 was added per well to dissolve formazan crystals. According to kit instructions, the plate was read in a microplate absorbance reader (Agilent Bio Tek Cytation Instruments, WI, USA). The cell viability percentages were obtained with Eq. (3).

$$Sampleviability\% = \left(\frac{sampleabsorbance}{negativecontrolabsorbance}\right) \times 100 \quad (3)$$

An analysis of variance (ANOVA) and Tukey's HSD (Honestly Significant Difference) test, with a confidence interval

of 95%, were performed to determine significant differences between the control group and the tested samples.

Cytotoxicity: H&E Staining

The MSC were seeded per well in a 96-well microplate, a total of 10,000 MSC. Cells were cultured and exposed to films same as the MTT assay. A hematoxylin and eosin (H&E) staining was performed according to ISO-10993-5. The culture media was removed, and cells were washed with PBS solution (Thermo Fisher Scientific, Waltham, MA, USA) three times. The cells were incubated for 10 min at −20 °C with cold methanol initiating the fixation procedure. Subsequently, cells were rewashed with PBS three times to eliminate methanol residuals. For the stain, the incubated cells were placed in hematoxylin for 5 min. Then, these were washed (two cycles) with distilled water and HCl (diluted at 0.5% in ethanol). Immediately, eosin was placed for 5 min, and finally, the cells were distilled water washed. The morphology of the cells was analyzed in an optical microscope (Inverted microscope CKX41, Olympus, Shinjuku, Japan).

Hemolysis Test

A hemolysis test was performed following the Standard Practice for Assessment of Hemolytic Properties of Materials ASTM F756-17 to measure the impact of erythrocyte lysis that the EPS1, EPS2, EPS3, PLA5, and PLA15 films can produce. A trained health worker took 3 mL of a blood sample from a healthy donor into a heparin tube utilizing venipuncture (Becton Dickinson, Franklin Lakes, NJ, USA). It is important to note that biosecurity parameters were taken into account. Erythrocytes were separated by centrifugation (3000 rpm for 4 min) and washed thrice with PBS solution. A final solution of 1% v/v of erythrocytes in PBS was prepared.

Moreover, each film's circular pieces (6 mm diameter) were sterilized with UV light exposition for 15 min on each side. The films were incubated in microtubes, by quadruplicate, in 200 µL of the 1% v/v erythrocytes solution for 30 min, at 37 °C and 400 rpm. An erythrocytes solution (1% v/v) was taken as a negative control (NC), not exposed to films. An erythrocytes solution in distilled water (1% v/v) was taken as a positive control (PC). After incubating samples and controls, tubes were centrifuged at 14,000 rpm for 3 min. Hemoglobin released in the supernatant was measured by UV–Vis spectroscopy (NanoDrop, Thermo Fisher Scientific Waltham, MA, USA) at 415 nm. The percentage of hemolysis was obtained with Eq. (4).

$$Hemolysis\% = \frac{(Sample_{abs} - NC_{abs})}{(PC_{abs} - NC_{abs})} \times 100 \quad (4)$$

Results and Discussion

The polymeric blends, namely EPS1, EPS2, and EPS3, have identical compositions; however, they differ in the mixing time and the order of the polymer's addition. The mixing time for EPS1 is 5 min, comparable with neat PLA5. The EPS2 and EPS3 samples have a mixing time of 15 min compared to neat PLA15. As for the order of the polymer's addition, EPS1 and EPS2 have identical methods; in contrast, EPS3 was formulated by mixing PLA and EVA for 10 min, and then SMMA was added, mixing them for 5 min completing 15 min.

Water Absorption and Remaining Mass

The impact of the hydrolytic degradation on EPS1, EPS2, and EPS3 blends was investigated. Since water absorption and remaining mass are intimately related to hydrolytic degradation were monitored for 168 days. Figure 2 illustrates hydrolytic degradation behavior regarding time (Fig. 2a). As noted for the first 7 days, the liquid absorption increased rapidly, Fig. 2a, reaching a maximum of 0.83% for the neat PLA15 sample. Subsequently, the absorption rate decreases until it increases after 28 days of immersion. At the end of 84 days, the EPS1 and EPS2 blends reported the

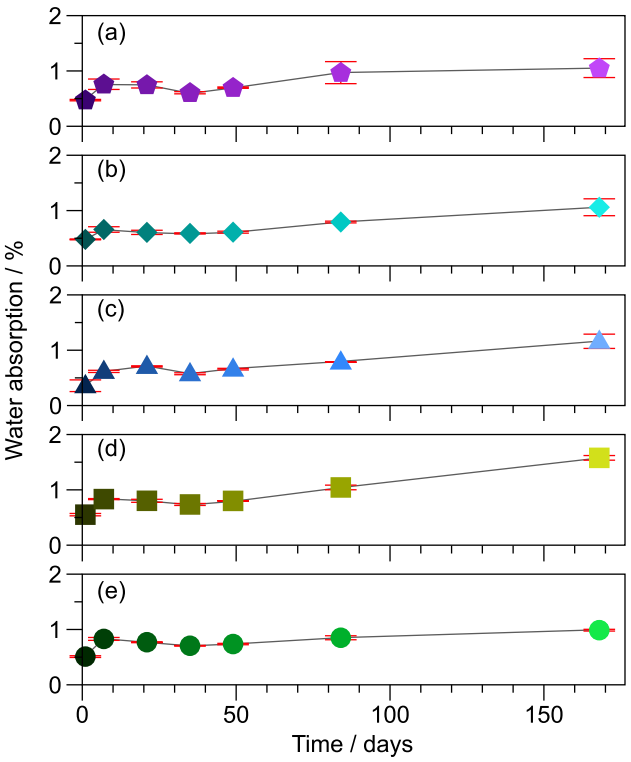

Fig. 2 Evolution of water absorption during hydrolytic degradation. **a** EPS3, **b** EPS2, **c** EPS1, **d** PLA15, and **e** PLA5

lowest percentage of water absorption, with values of 0.78% and 0.79%, respectively. Nevertheless, the PLA15 sample reported the highest amount of water absorption, around 1.04% at 168 days (Fig. 2a).

Singla et al. [45] studied PLA/EVA blends and mentioned that the presence of EVA droplets in the PLA facilitates water diffusion in the PLA/EVA interface. Nevertheless, in this study, SMMA lies between PLA and EVA bubbles hindering the water diffusion inside the sample, according to our previous work [34].

Additionally, it is well known that water absorption in PLA accelerates hydrolysis due to the cleavage of ester bonds [46]. The degradation property and velocity have also been related to this phenomenon [47]. Liu et al. reported that PLLA scaffolds undergo a first period of degradation, where PLLA absorbs a volume of the PBS solution, allowing swelling and subsequent hydrolytic degradation of the lower molecular weight PLLA. In addition, the gradual increase in the amount of liquid absorbed generates defects and porosity [31].

The results of the remaining mass (R_{mass}) are illustrated in Fig. 3; according to Eq. 2. The general changes presented by the samples are insignificant, with a variation of ±1%. However, the comparison of polymer blends reveals that EPS1 and EPS2 blends recorded the lowest weight increase than EPS3. In our previous work [34],

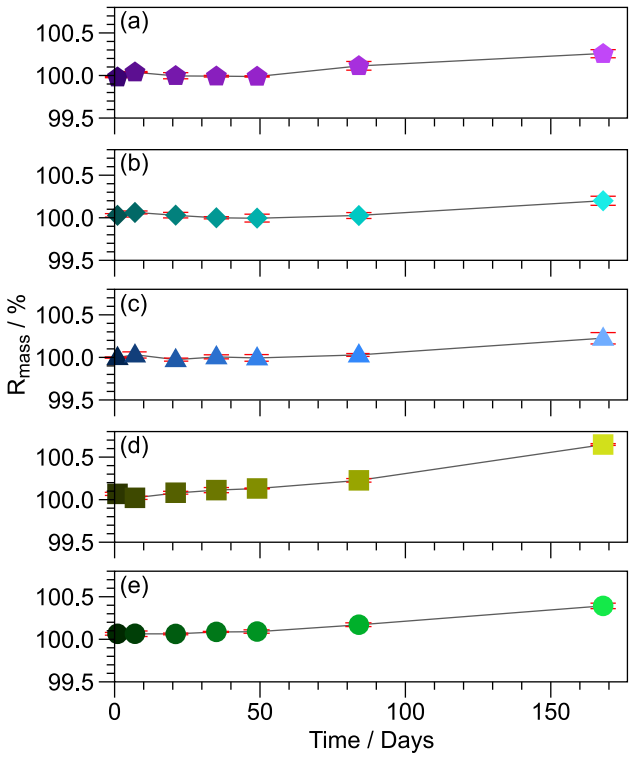

Fig. 3 Remaining mass of the samples. **a** EPS3, **b** EPS2, **c** EPS1, **d** PLA15, and **e** PLA5

EPS1 and EPS2 morphologically exhibited a homogeneity in EVA microbubbles suggesting that longer processing time is needed, as well as adding SMMA at the commencement of mixing formulation. In contrast, the morphology of EVA for EPS3 is considerably heterogeneous due to the coalescence process, which leads to higher water absorption than EPS1 and EPS2. This result can be explained by the formation of EVA bubbles, inhibiting the water diffusion towards the inside of the test probe, thereby slowing the degradation rate. Wongwiwattana and Thomas [33] observed a similar behavior because most degradation reaction products remain inside the samples. Likewise, in this study, it is observed that the PLA15 sample gains weight in a more significant proportion, considered as an example at 84 days, a value around 0.22%, compared to the EPS blends. This behavior suggests that PLA undergoes a faster hydrolytic degradation rate than EPS mixtures because they contain EVA and SMMA.

Additionally, there are studies of PLA degradability utilizing phosphate solutions at 37 °C with results different from this study; notwithstanding, the measurement methodology is distinct. Navarro et al. [32] reported no weight loss in PLA/PCL blends with a PLA content between 70 and 100%, even after 140 days of hydrolytic degradation, while blends with lower content of PLA lose a 3 wt% after 140 days. Nevertheless, they changed the PBS solution once a week. Wongwiwattana and Thomas [33] reported that blends with PLA do not degrade because their glass transition temperature is above 37 °C and is too low to cause a significant hydrolysis reaction since the reaction is limited to the diffusion of PBS into the samples. Likewise, it is reported that PLA commonly presents hydrolysis at temperatures higher than 50 °C [7, 48]. Navarro et al. [32] also mentioned that PLA degrades by chain scission across the hole polymer chains; however, they remained inside and did not disappear during the washing of the sample, originating no weight loss. Other investigations have reported that the degradation process of PLA is by hydrolytic degradation of the ester group, and the subproducts of this degradation can be assimilated [49, 50].

To summarize, the minor changes in the remaining mass of the EPS1, EPS2, and EPS3 blends can be explained due to the low rate of hydrolytic degradation occurring at 37 °C, and the PBS solution was not changed over time.

pH

The hydrolytic degradation of the PLA and EPS blends was investigated by measuring the pH of the PBS solution at different times, Fig. 4. The behavior of the physicochemical property pH is a decrease close to 0.4 until day 49. It is well known that the byproducts of the hydrolytic degradation of

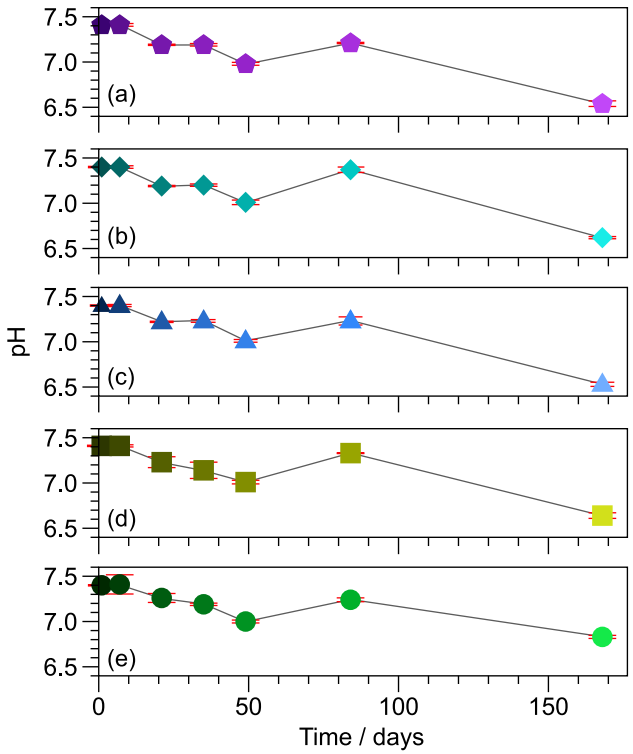

Fig. 4 Evolution of pH during hydrolytic degradation. **a** EPS3, **b** EPS2, **c** EPS1, **d** PLA15, **e** PLA5

PLA are functional groups of carboxylic acid type; therefore, the pH diminishes [51, 52]. However, Gorrasi and Pantani [24] observed a pH increment on amorphous and semicrystalline PLA in the first 6 days, followed by a decrease depending on the D isomer content, suggesting an acid-based hydrolysis mechanism. In addition, hydrolysis degradation tests were carried out in distilled water with a pH of 5.7 and at 58 °C.

The pH, at 84 days, presented a gradual increase, reaching a value of around 7.37 and 7.33 for the EPS2 blend and PLA15, respectively. In contrast, at 168 days, the pH of the PBS solutions was reduced. For example, the solution corresponding to the samples EPS1, EPS2, and EPS3 registered an acidity between 6.5 and 6.6. According to Gorrasi and Pantani [24], PLA hydrolysis can occur in three phases: (1) diffusion of H_3O^+ in the polymeric bulk, that is, an excess of OH^- in the solution, which would justify the increase in pH; (2) hydrolysis reaction, and (3) counter diffusion of reaction products (carboxylic acids, alcohols, oligomers). Therefore, the observed changes in pH at day 84 could be attributed to the beginning of OH^- production at this time of the hydrolytic degradation test.

Scanning Electron Microscopy

Physical degradation of polymers can develop in two ways: bulk or surface erosion. Bulk erosion is when degradation proceeds throughout the polymer matrix, while surface erosion is located only on the polymer surface [25, 53, 54]. Figure 5 illustrates the surface morphologies of PLA5, PLA15, EPS1, EPS2, and EPS3 samples at 0, 49, and 168 days of hydrolytic degradation. All micrographs of the samples at different times are observed in the supplementary material. Compared with the neat PLA5 at day 0, the samples of neat PLA5 at 49 and 168 days present a smoother surface (Fig. 5a–c). In addition, on day 168, slight flaking is observed, which can be attributed to the beginning of the polymer degradation. As can be observed, the neat PLA15 sample presents higher roughness (Fig. 5d–f), as well as the generation of small holes over its surface since day 49 (Fig. 5e), which is attributable to surface erosion. On day 168, these holes transform into cracks and are more prominent, suggesting higher degradation.

Moreover, the EPS blends show differences in surface morphology when compared regarding time, see Fig. 5g–o. For example, on day 49, EPS2 and EPS3 show holes on the surface; on the contrary, EPS1 has a smoother surface suggesting that this blend was degraded to a minimal grade. In the same way, it is observed at 168 days. These results can be explained by the processing conditions used to obtain the probes. The EPS1 blend has the shortest mixing time compared to the 15 min of EPS2 and EPS3. Hence, a mixing time of 5 min is necessary to decrease the hydrolytic degradation of the PLA blend.

In order to analyze the morphology of the cross-section during hydrolytic degradation, the probes were fractured with liquid nitrogen. Figure 6 illustrates the micrographs of PLA and EPS blends during hydrolytic degradation. The formation of holes is evident on day 168 for the neat PLA5 and PLA15 (Fig. 6a–f). Compared with neat PLA5, the PLA15 sample exhibits numerous pores evenly distributed throughout the probe, suggesting more bulk hydrolytic degradation. Zamani et al. [55] reported that degradation occurs at the surface when the degradation rate of the polymer is faster than the permeation rate of the solvent into the polymer matrix. Otherwise, degradation will take place inside the polymer matrix. Furthermore, Tsuji et al. [56] mention that the bulk erosion mechanism of PLA is dominant when hydrolyzed in PBS (pH 7.4).

Additionally, some authors mention that the hydrolytic degradation of amorphous poly (DL-lactic acid) proceeds heterogeneously and is faster inside than on the surface since a more significant contribution of autocatalysis occurs [57–59]. This behavior is consistent with our water absorption results, see Fig. 2. In previous work, a representative model of EPS blends was described, illustrating the role of

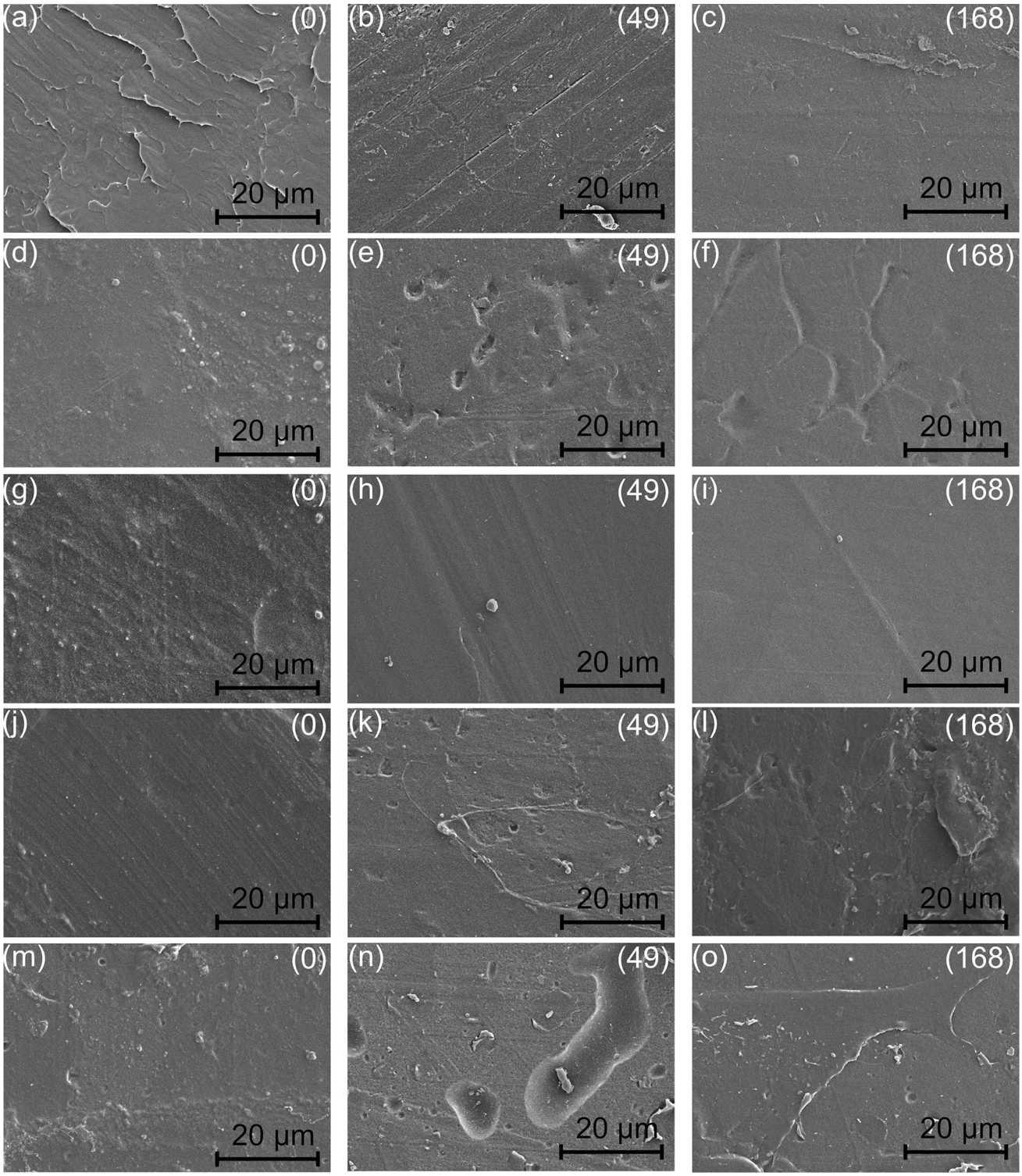

Fig. 5 Surface scanning electron micrographs of PLA and EPS blends at (0), (49), and (168) days of exposure to PBS solution at 37 °C. **a–c** PLA5; **d–f** PLA15; **g–i** EPS1; **j–l** EPS2; **m–o** EPS3

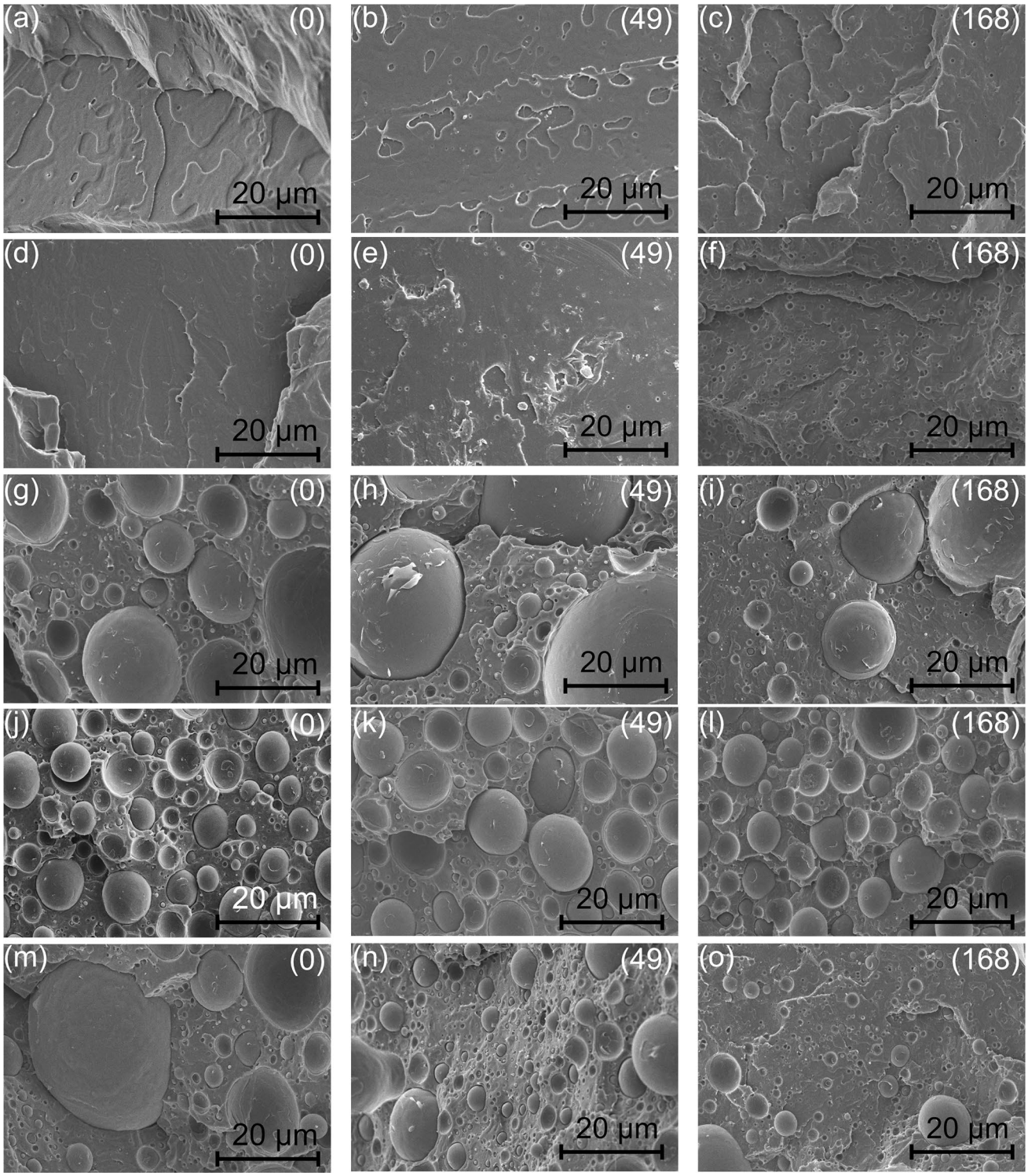

Fig. 6 Cross-section scanning electron micrographs of PLA and EPS blends at (0), (49), and (168) days of exposure to PBS solution at 37 °C. **a–c** PLA5; **d–f** PLA15; **g–i** EPS1; **j–l** EPS2; **m–o** EPS3

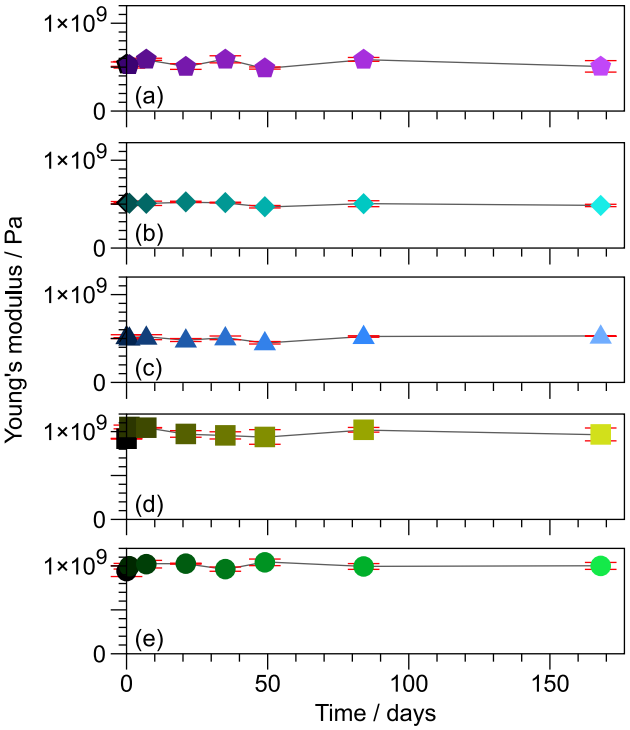

Fig. 7 Young's modulus behavior during hydrolytic degradation. **a** EPS3, **b** EPS2, **c** EPS1, **d** PLA15, **e** PLA5

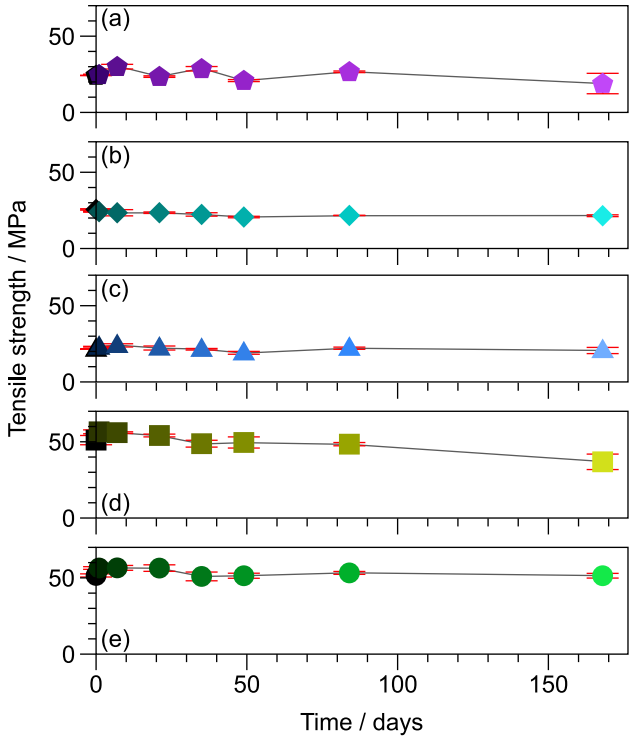

Fig. 8 Tensile strength during hydrolytic degradation. **a** EPS3, **b** EPS2, **c** EPS1, **d** PLA15, **e** PLA5

each component in the ternary blend coexistence [34]. Concerning EPS1 (Fig. 6g–i), the small pores become evident after 49 days of degradation. In the case of EPS2 (Fig. 6j–l), fewer pores are observed on day 168, attributed to the homogeneity in size and distribution of EVA microbubbles generated during processing [6]. This homogeneity hinders the diffusion of the liquid inside the probe, decreasing the degradation rate of the bulk material.

Mechanical Evaluation

The mechanical properties of the PLA and EPS blends were evaluated during hydrolytic degradation, specifically elastic modulus (E), tensile strength (TS), and elongation at break. Figure 7 displays the E of the PLA5, PLA15, EPS1, EPS2, and EPS3 samples. In the EPS blends (Fig. 7a–c), at time 0, the values of E were similar, around 0.52 GPa. However, on day 49, the samples EPS1, EPS2, and EPS3 show a decrease in modulus E of 13%, 10%, and 6%, respectively. It is important to note that at 49 days was recorded that the mixtures began to retain saline liquid, which could be related to this decrease in E. In the case of PLA5, no significant affectation was observed in E throughout the test. However, the PLA15 sample consistently displayed lower modulus values than the neat PLA5 sample, indicating a more significant degradation acquired during the processing of PLA for a longer time, 15 min.

Figure 8 displays the TS in tension measured at different hydrolytic degradation times of all samples. TS represents the probe's resistance to elongation [60]. All EPS blends report lower values of TS than PLA (Fig. 8a–e), attributed to the EVA content in the blend. TS presents more fluctuations for EPS blends during the hydrolytic degradation than PLA. These results could be associated with the heterogeneous morphology of EPS blends mainly caused by EVA bubbles.

Additionally, TS was more affected for PLA15 compared to day 168. In addition, the neat PLA15 sample presented a stress value of 27% lower than neat PLA5 at the end of the degradation test. This result could be due to a substantial amount of water absorption, which favors the degradation of the material and hence mechanically deteriorates PLA15 in a significant proportion favoring the sliding of the polymeric chains. However, compared with neat PLA5 on day 0, the neat PLA15 exhibits slightly lower TS due to a degradation of the polymer during the mixing and molding process. In particular, the neat PLA15 presented a lower viscosity than the neat PLA5 indicating a more significant degradation due to a shortening of polymer chains. The viscosity analysis was done in our previous work [34]. This shortening can also facilitate liquid diffusion into the material, thereby lowering mechanical performance. According to Rosli and coworkers [61], when the PLA is in an amorphous state, it allows a

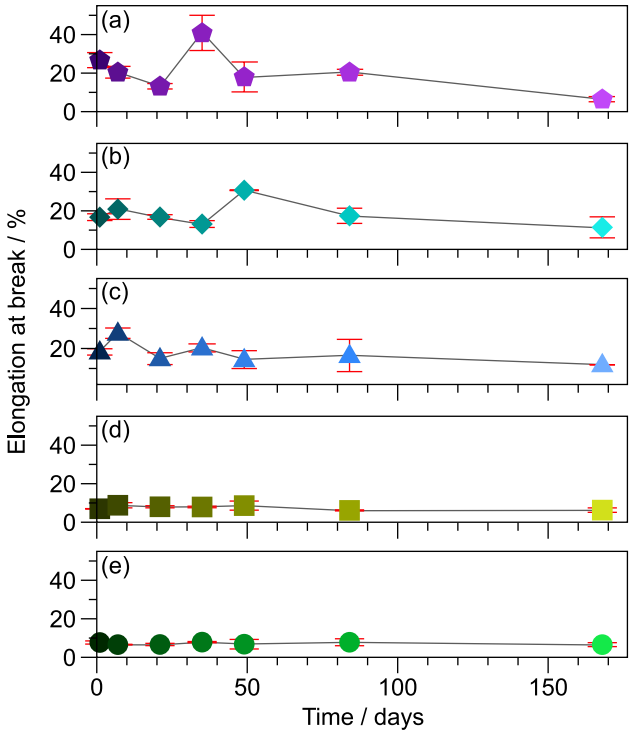

Fig. 9 Elongation at break behavior during hydrolytic degradation. **a** EPS3, **b** EPS2, **c** EPS1, **d** PLA15, **e** PLA5

considerable diffusion of water inside the polymer, causing a faster degradation and, therefore, a decrease in mechanical properties.

The elongation at break of the PLA and EPS blends is displayed in Fig. 9. The EPS3 blend reported the lowest elongation percentage at time zero regarding the EPS blends, see Fig. 9a–c. As the degradation test elapsed, the elongation percentage had erratic behavior. However, on day 168, all blends reported lower elongation values than those reported on day 0. Likewise, the EPS3 sample had the lowest elongation on day 168, showing a more brittle behavior due to degradation. Furthermore, EPS2 displayed higher mechanical stability during hydrolytic degradation. This finding can be attributed to less bulk degradation, as observed by microscopy. Equally important is the processing conditions of this blend, especially 15 min of mixing all its components. On the other hand, the fluctuations in elongation at break could be attributed to differences in morphology acquired during sample processing. As previously observed by microscopy EPS blends present differences in the homogeneity in size and distribution of EVA microbubbles generated during processing, which are the main contributor to the elongation capacity of the blends. For some medical applications, such as drug delivery, surface degradation is more desirable because it permits the delivery of the drug to maintain the

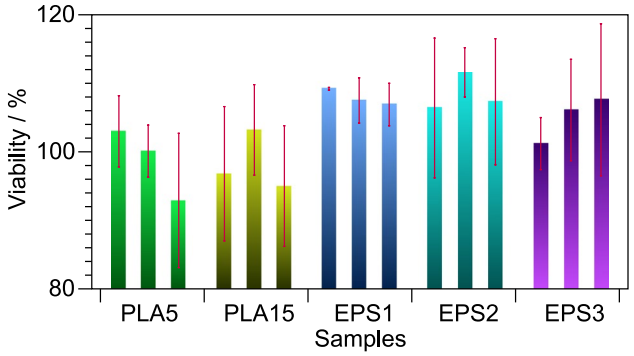

Fig. 10 MMT results of PLA and EPS blends

mechanical integrity of the material [62], as in the case of EPS2.

The PLA15 sample reports appreciable elongation from 0 to 49 degradation days. This result can be attributed to the fact that, as previously mentioned, this sample suffered considerable degradation during processing. Therefore, its polymeric chains are smaller, which could favor movement when the sample is stressed, resulting in significant elongation. However, on days 84 and 168, PLA15 reported the lowest elongation caused by a higher rate of water absorption, i.e., a higher rate of degradation. Finally, PLA5 (Fig. 9e) did not present significant changes during hydrolytic degradation.

Vieira et al. [52] reported a negligible variation in Young's modulus of the fibers, in PLA-PCL fibers, during the degradation process with saline phosphate solution at pH 7.4 and a temperature of 37 °C. Likewise, Zhou et al. [63] studied mixtures of polybutylene succinate with PLA subjected to hydrolytic degradation in a solution simulating human body fluids at a pH of 7.4 and a temperature of 37 °C. They reported no statistical difference in the tensile strength of PLA until about 6 months of degradation and reported 60% in mechanical strength, indicating that PLA experiences slower degradation compared to PBS. Additionally, they mention that elongation at break is the most sensitive index for monitoring the anchorages of the polymeric chains.

Possible applications are the manufacture of tendons and ligaments and as a replacement for the porous part of the bone (also called trabecular or spongy bone). Tensile strength from 4.4 to 660 MPa for ligaments and tendons of different parts of the human body was reported [64–66]. Regarding the maximum deformation and Young's modulus of these connective tissues, values between 18 and 30% and 0.2 to 1.5 GPa were found, respectively [67, 68]. Specifically, in trabecular bones, which constitute the porous or spongy part of the bones, the modulus of elasticity ranges from 0.02 GPa to 0.5 GPa [69, 70].

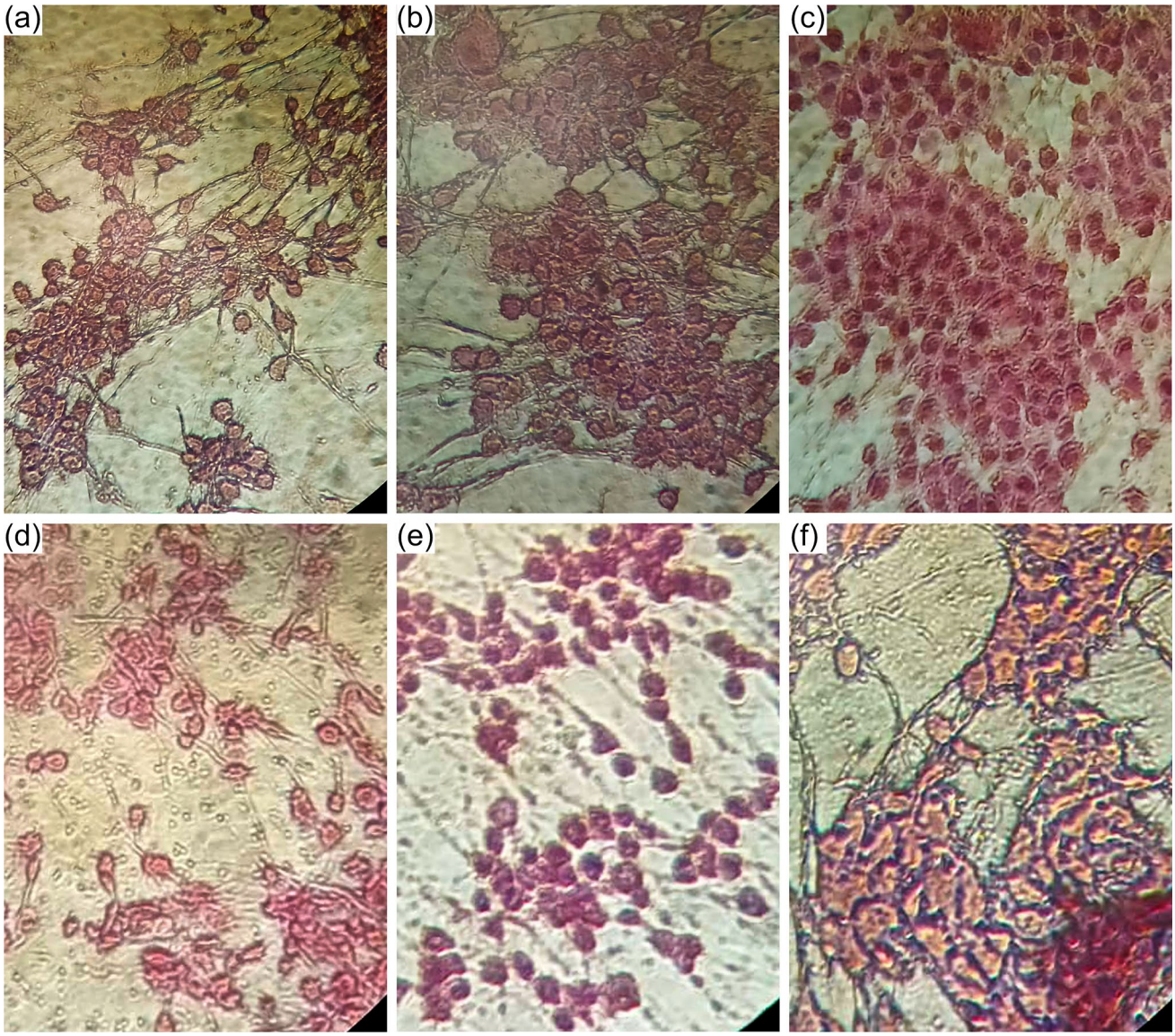

Fig. 11 Optical microscope images at 40× of H&E staining at 24 h. **a** Negative control, **b** PLA5, **c** PLA15, **d** EPS1, **e** EPS2, **f** EPS3

Evaluation of the Cytotoxicity

Cytotoxicity tests evaluate cell damage, growth, and metabolism. MTT assay measures the metabolic activity of cells. The results of the MMT assay are shown in Fig. 10. The materials tested showed no statistical difference ($p = 0.05$) compared with the negative control, which can be considered that there is no evidence of damage in the cell metabolism. Therefore, EPS blends should not be considered dangerous substances.

The proliferation of mesenchymal cell growth in PLA and PCL nanofibrous scaffolds has previously been studied by Marei et al. [71]. They established that the cytotoxicity of both polymers was negligible because BMSC showed similar cell viability at day 3 compared to the control group.

To observe morphological changes in the cells due to their exposure to EPS blends and their comparison with neat PLA and negative control, H&E was performed. Figure 11 shows images from an optical microscope at 40× after 24 h of exposure. Cell morphology changes and cell confluence alterations were not observed in the evaluated samples. In addition, there are no evident changes in the cytoplasm or nucleus morphology. H&E results are comparable with MMT results, with both assays showing no evident cell damage.

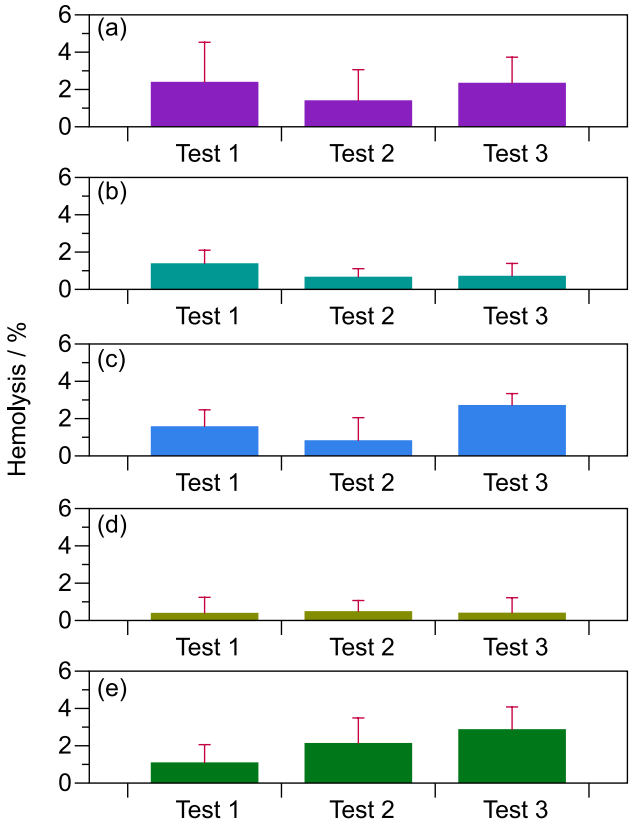

Fig. 12 Hemolysis results. **a** EPS3, **b** EPS2, **c** EPS1, **d** PLA15, **e** PLA5

Evaluation of the Hemolysis

Hemolysis assay involves exposing the material to erythrocytes recently extracted from the human body. Red blood cells are sensitive, and their membrane will lyse if the materials are incompatible. The percentage of hemolysis can be measured because the erythrocytes have hemoglobin inside them. All erythrocytes that have been lysed will release hemoglobin, which spectroscopy UV–Vis measure at 415 nm. Compatible materials will not lyse erythrocytes; therefore, no hemoglobin will be released into the medium.

Hemolysis assays are a reference to know if biomaterials present some toxicity levels. Biomaterials must not produce cellular damage to any components, including membranes. Membrane lysis can be measured by hemolysis assay in human erythrocytes. In this assay, hemoglobin is released at the medium when the outer membrane of the human erythrocytes is destroyed. Lysis produces the release of all the intracellular content from the red cells. The measurement of released hemoglobin estimates the number of erythrocytes destroyed. The Standard Practice analyzed the results for Assessment of Hemolytic Properties of Materials ASTM F756-08, which indicates that any material with a hemolysis rate of less than 5% is not considered high hemolytic [72]. All the tested samples are below 5% hemolysis, Fig. 12; therefore, none of the materials are considered hemolytic. However, some of them are above 2%, indicating they are low hemolytic, so this must be considered to propose a relevant medical application. However, the PLA5 also exceeded the value of 2% in two of its specimens. Since PLA is a material considered suitable for medical applications, if we take the value of this last material as a reference, all the samples could be used without problems in developing a medical device in terms of cytotoxicity.

Conclusions

The hydrolytic degradation study demonstrated that the ternary samples reported less absorbed water than the neat PLA. This result suggests that the incorporation of EVA and SMMA into the PLA matrix retards its rate of hydrolytic degradation, providing the possibility of having control of this type of degradation. The highest hydrolytic degradation was observed in the PLA15 sample, suggesting that longer mixing time favors the PLA molecule's scissions and hence its hydrolytic degradation.

The elastic modulus and tensile strength did not register significant variations in any sample during the entire hydrolytic degradation test, except in the case of PLA15, which experimented a decrease in tensile strength from 51.09 MPa to 36.86 MPa from day 0 to 168, respectively. This finding could be due to a substantial amount of water absorption, which favors the degradation of the material and hence mechanically deteriorates PLA15 in a significant proportion favoring the sliding of the polymeric chains.

Concerning elongation at break, it presented fluctuations during the 168 days of testing owing to sample morphology and the processing conditions. In addition, this property was the most sensitive to hydrolytic degradation. Compared with EPS1 and EPS2, EPS3 showed the lowest elongation at break on day 168, with a value of 6.46%. In contrast, EPS2 had a stable mechanical performance during hydrolytic degradation. This behavior can be attributed to a more homogeneous morphology acquired, where all components were mixed for 15 min. Compared with the samples, PLA15 displayed the lowest elongation at break on days 84 and 168, 6.13%, and 6.28%, respectively, due to higher water absorption.

Biocompatibility tests showed that EVA/PLA/SMMA blends showed no statistical difference compared with the negative control, which makes them non-toxic. EPS blends presented good hemocompatibility with values of less than 5%, considered an acceptable limit.

Supplementary Information The online version contains supplementary material available at https://doi.org/10.1007/s10924-023-03019-1.

Acknowledgements Mónica Mendoza Duarte would like to acknowledge the Universidad Autónoma de Ciudad Juárez (UACJ), Universidad Autónoma de Nuevo León (UANL) and Centro de Investigación en Materiales Avanzados (CIMAV) for the facilities provided for this investigation. The authors would also like to thank Luis de la Torre Sáenz and Roberto Bernal González for their technical assistance and the Laboratorio Nacional de Nanotecnología (Nanotech), especially to Karla Campos Venegas for technical support in SEM images acquisition.

Author contributions MM: Conceptualization, Methodology, Investigation, Writing—original draft, Writing—review and editing. JR: Methodology (MSC Primary Culture, cytotoxicity and hemolysis tests), Investigation, Formal Analysis. AQ: Validation, Investigation. EG: Validation, Investigation. CS: Validation, Investigation. PG: Validation, Methodology, Writing—original draft. AV: Conceptualization, Validation, Formal analysis, Writing—original draft, Writing—review and editing, Supervision.

Funding This research was funded by the Centro de Investigación en Materiales Avanzados, SC, grant number PI-23-05/2023.

Declarations

Conflict of interest The authors declare no conflict of interest.

References

1. Banoriya D, Purohit R, Dwivedi RK (2017) Advanced application of polymer based biomaterials. Mater Today Proc 4:3534–3541. https://doi.org/10.1016/j.matpr.2017.02.244
2. Volova TG, Vinnik YS, Shisshatskaa EI, Markelova NM (2017) Natural-based polymers for biomedical applications. Apple Academic Press Inc., Oakvile, ON, Canada
3. Wang M, Wu Y, Li YD, Zeng JB (2017) Progress in toughening poly(lactic acid) with renewable polymers. Polym Rev 57:557–593. https://doi.org/10.1080/15583724.2017.1287726
4. Zhang S, Yan D, Zhao L, Lin J (2022) Composite fibrous membrane comprising PLA and PCL fibers for biomedical application. Compos Commun 34:101268. https://doi.org/10.1016/J.COCO.2022.101268
5. Soares JS, Moore JE, Rajagopal KR (2008) Constitutive framework for biodegradable polymers with applications to biodegradable stents. ASAIO J 54:295–301. https://doi.org/10.1097/MAT.0b013e31816ba55a
6. Tamai H, Igaki K, Kyo E, Kosuga K, Kawashima A, Matsui S, Komori H, Tsuji T, Motohara S, Uehata H (2000) Initial and 6-month results of biodegradable poly-L-lactic acid coronary stents in humans. Circulation 102:399–404. https://doi.org/10.1161/01.CIR.102.4.399
7. Farah S, Anderson DG, Langer R (2016) Physical and mechanical properties of PLA, and their functions in widespread applications—a comprehensive review. Adv Drug Deliv Rev 107:367–392. https://doi.org/10.1016/j.addr.2016.06.012
8. Saini P, Arora M, Kumar MNVR (2016) Poly(lactic acid) blends in biomedical applications. Adv Drug Deliv Rev 107:47–59. https://doi.org/10.1016/j.addr.2016.06.014
9. Ulery BD, Nair LS, Laurencin CT (2011) Biomedical applications of biodegradable polymers. J Polym Sci B Polym Phys 49:832–864. https://doi.org/10.1002/polb.22259
10. Lim JY, Kim SH, Lim S, Kim YH (2003) Improvement of flexural strengths of poly(L-lactic acid) by solid-state extrusion, 2: extrusion through rectangular die. Macromol Mater Eng 288:50–57. https://doi.org/10.1002/mame.200290033
11. Mao D, Li Q, Li D, Chen Y, Chen X, Xu X (2018) Fabrication of 3D porous poly(lactic acid)-based composite scaffolds with tunable biodegradation for bone tissue engineering. Mater Des 142:1–10. https://doi.org/10.1016/j.matdes.2018.01.016
12. Bahraminasab M, Janmohammadi M, Arab S, Talebi A, Nooshabadi VT, Koohsarian P, Nourbakhsh MS (2021) Bone scaffolds: an incorporation of biomaterials, cells, and biofactors. ACS Biomater Sci Eng 7:5397–5431. https://doi.org/10.1021/acsbiomaterials.1c00920
13. Middleton JC, Tipton AJ (2000) Synthetic biodegradable polymers as orthopedic devices. Biomaterials 21:2335–2346. https://doi.org/10.1016/S0142-9612(00)00101-0
14. Savioli Lopes M, Jardini AL, Maciel Filho R (2012) Poly (lactic acid) production for tissue engineering applications. Procedia Eng 42:1402–1413. https://doi.org/10.1016/j.proeng.2012.07.534
15. Hamad K, Kaseem M, Yang HW, Deri F, Ko YG (2015) Properties and medical applications of polylactic acid: a review. Express Polym Lett 9:435–455. https://doi.org/10.3144/expresspolymlett.2015.42
16. Haers PE, Suuronen R, Lindqvist C, Sailer H (1998) Biodegradable polylactide plates and screws in orthognathic surgery: technical note. J Craniomaxillofac Surg 26:87–91. https://doi.org/10.1016/S1010-5182(98)80045-0
17. Ebrahimi F, Ramezani Dana H (2022) Poly lactic acid (PLA) polymers: from properties to biomedical applications. Int J Polym Mat Polym Biomater 71:1117–1130. https://doi.org/10.1080/00914037.2021.1944140
18. Tyler B, Gullotti D, Mangraviti A, Utsuki T, Brem H (2016) Polylactic acid (PLA) controlled delivery carriers for biomedical applications. Adv Drug Deliv Rev 107:163–175. https://doi.org/10.1016/j.addr.2016.06.018
19. Sheikh Z, Najeeb S, Khurshid Z, Verma V, Rashid H, Glogauer M (2015) Biodegradable materials for bone repair and tissue engineering applications. Materials 8:5744–5794. https://doi.org/10.3390/MA8095273
20. Velioglu ZB, Pulat D, Demirbakan B, Ozcan B, Bayrak E, Erisken C (2019) 3D-printed poly(lactic acid) scaffolds for trabecular bone repair and regeneration: scaffold and native bone characterization. Connect Tissue Res 60:274–282. https://doi.org/10.1080/03008207.2018.1499732
21. ASTM F 756-00 (2000) Standard practice for assessment of hemolytic properties of materials. Philadelphia
22. Huttunen M, Kellomäki M (2013) Strength retention behavior of oriented PLLA, 96L/4D PLA, and 80L/20D, L PLA. Biomatter 3:37–41. https://doi.org/10.4161/biom.26395
23. Ishii D, Ying TH, Mahara A, Murakami S, Yamaoka T, Lee WK, Iwata T (2009) In vivo tissue response and degradation behavior of PLLA and stereocomplexed PLA nanofibers. Biomacromol 10:237–242. https://doi.org/10.1021/bm8009363

24. Gorrasi G, Pantani R (2013) Effect of PLA grades and morphologies on hydrolytic degradation at composting temperature: assessment of structural modification and kinetic parameters. Polym Degrad Stab 98:1006–1014. https://doi.org/10.1016/j.polymdegradstab.2013.02.005
25. Wei Z, Wang W, Zhou C, Jin C, Leng X, Li Y, Zhang X, Chen S, Zhang B, Yang K (2020) In vitro degradation and biocompatibility evaluation of fully biobased thermoplastic elastomers consisting of poly(β-myrcene) and poly(L-lactide) as stent coating. Polym Degrad Stab 179:109254. https://doi.org/10.1016/j.polymdegradstab.2020.109254
26. Yao Q, Cosme JGL, Xu T, Miszuk JM, Picciani PHS, Fong H, Sun H (2017) Three dimensional electrospun PCL/PLA blend nanofibrous scaffolds with significantly improved stem cells osteogenic differentiation and cranial bone formation. Biomaterials 115:115–127. https://doi.org/10.1016/J.BIOMATERIALS.2016.11.018
27. Yeo JCC, Lin TT, Koh JJ, Low LW, Tan BH, Li Z, He C (2021) Insights into the nucleation and crystallization analysis of PHB-rubber toughened PLA biocomposites. Compos Commun 27:100894. https://doi.org/10.1016/J.COCO.2021.100894
28. Li G, Zhao M, Xu F, Yang B, Li X, Meng X, Teng L, Sun F, Li Y (2020) Synthesis and biological application of polylactic acid. Molecules 25:5023. https://doi.org/10.3390/MOLECULES25215023
29. Murariu M, Arzoumanian T, Paint Y, Murariu O, Raquez J-M, Dubois P (2022) Engineered polylactide (PLA)–polyamide (PA) blends for durable applications: 1. PLA with high crystallization ability to tune up the properties of PLA/PA12 blends. Eur J Mater 2022:1–36. https://doi.org/10.1080/26889277.2022.2113986
30. Ishaque N, Naseer N, Abbas MA, Javed F, Mushtaq S, Ahmad NM, Khan MFA, Ahmed N, Elaissari A (2022) Optimize PLA/EVA polymers blend compositional coating for next generation biodegradable drug-eluting stents. Polymers (Basel) 14:1–14. https://doi.org/10.3390/polym14173547
31. Liu YS, Huang QL, Kienzle A, Müller WEG, Feng QL (2014) In vitro degradation of porous PLLA/pearl powder composite scaffolds. Mater Sci Eng C 38:227–234. https://doi.org/10.1016/J.MSEC.2014.02.007
32. Navarro-Baena I, Sessini V, Dominici F, Torre L, Kenny JM, Peponi L (2016) Design of biodegradable blends based on PLA and PCL: from morphological, thermal and mechanical studies to shape memory behavior. Polym Degrad Stab 132:97–108. https://doi.org/10.1016/j.polymdegradstab.2016.03.037
33. Wongwiwattana P, Thomas NL (2021) Co-continuous phase prediction in poly(lactic acid) /poly(caprolactone) blends from melt viscosity measurements. Polym Plastics Technol Mater 60:1393–1410. https://doi.org/10.1080/25740881.2021.1904983
34. Mendoza-Duarte ME, Estrada-Moreno IA, García-Casillas PE, Vega-Rios A (2021) 2 stiff-elongated balance of PLA-based polymer blends. Polymers 13:4279. https://doi.org/10.3390/polym13244279
35. Lim WLY, Azizul Rahim FH, Johar M, Rusli A (2022) Tensile and shape memory properties of polylactic acid/ethylene–vinyl acetate blends. Mater Today Proc 66:2771–2775. https://doi.org/10.1016/j.matpr.2022.06.513
36. Kugimoto D, Kouda S, Yamaguchi M (2019) Improvement of mechanical toughness of poly(lactic acid) by addition of ethylene–vinyl acetate copolymer. Polym Test 80:106021. https://doi.org/10.1016/j.polymertesting.2019.106021
37. Mc Conville C, Major I, Friend DR, Clark MR, Woolfson AD, Malcolm RK (2012) Development of polylactide and polyethylene vinyl acetate blends for the manufacture of vaginal rings. J Biomed Mater Res B Appl Biomater 100B:891–895. https://doi.org/10.1002/jbm.b.31919
38. Zuo X, Xue Y, Wang L, Zhou Y, Yin Y, Chuang YC, Chang CC, Yin R, Rafailovich MH, Guo Y (2019) Engineering styrenic blends with poly(lactic acid). Macromolecules 52:7547–7556. https://doi.org/10.1021/acs.macromol.9b01349
39. Solorio L, Vega A (2019) Filament extrusion and its 3D printing of poly(lactic acid)/poly(styrene-*co*-methyl methacrylate) blends. Appl Sci 9:1–17. https://doi.org/10.3390/app9235153
40. Liu X, Lei L, Hou J-W, Tang M-F, Guo S-R, Wang Z-M, Chen K-M (2011) Evaluation of two polymeric blends (EVA/PLA and EVA/PEG) as coating film materials for paclitaxel-eluting stent application. J Mater Sci Mater Med 22:327–337. https://doi.org/10.1007/s10856-010-4213-3
41. Le KP, Lehman R, Remmert J, Vanness K, Ward PML, Idol JD (2006) Multiphase blends from poly(L-lactide) and poly(methyl mathacrylate). J Biomater Sci Polym Ed 17:121–137. https://doi.org/10.1163/156856206774879054
42. Mihai M, Canada C (2017) Extrusion foaming of polylactide. In: Polymeric foams: innovations in process, technologies, and products. CRC Press Taylor & Francis
43. ASTM D638 (2006) Standard test method for tensile properties of plastics 1
44. Oyama HT, Tanishima D, Maekawa S (2016) Poly(malic acid-*co*-L-lactide) as a superb degradation accelerator for poly(L-lactic acid) at physiological conditions. Polym Degrad Stab 134:265–271. https://doi.org/10.1016/j.polymdegradstab.2016.10.016
45. Singla RK, Zafar MT, Maiti SN, Ghosh AK (2017) Physical blends of PLA with high vinyl acetate containing EVA and their rheological, thermo-mechanical and morphological responses. Polym Test 63:398–406. https://doi.org/10.1016/J.POLYMERTESTING.2017.08.042
46. Zabihzadeh Khajavi M, Ebrahimi A, Mortazavian AM, Farhoodi M, Ahmadi S (2022) Hydrolytic degradation mechanism of modified polylactic acid in different food simulants. Food Packag Shelf Life 34:100956. https://doi.org/10.1016/j.fpsl.2022.100956
47. Cifuentes SC, Gavilán R, Lieblich M, Benavente R, González-Carrasco JL (2016) In vitro degradation of biodegradable polylactic acid/magnesium composites: relevance of Mg particle shape. Acta Biomater 32:348–357. https://doi.org/10.1016/j.actbio.2015.12.037
48. Auras R, Harte B, Selke S (2004) An overview of polylactides as packaging materials. Macromol Biosci 4:835–864. https://doi.org/10.1002/mabi.200400043
49. Vert M, Mauduit J, Li S (1994) Biodegradation of PLA/GA polymers: increasing complexity. Biomaterials 15:1209–1213. https://doi.org/10.1016/0142-9612(94)90271-2
50. Pluta M, Galeski A, Alexandre M, Paul M-A, Dubois P (2002) Polylactide/montmorillonite nanocomposites and microcomposites prepared by melt blending: structure and some physical properties. J Appl Polym Sci 86:1497–1506. https://doi.org/10.1002/app.11309
51. Revati R, Majid MSA, Ridzuan MJM, Basaruddin KS, Rahman MNY, Cheng EM, Gibson AG (2017) In vitro degradation of a 3D porous *Pennisetum purpureum*/PLA biocomposite scaffold. J Mech Behav Biomed Mater 74:383–391. https://doi.org/10.1016/j.jmbbm.2017.06.035
52. Vieira AC, Vieira JC, Ferra JM, Magalhães FD, Guedes RM, Marques AT (2011) Mechanical study of PLA–PCL fibers during in vitro degradation. J Mech Behav Biomed Mater 4:451–460. https://doi.org/10.1016/j.jmbbm.2010.12.006
53. Lim KS, Park JK, Jeong MH, Nah JW, Bae IH, Park DS, Shim JW, Kim JH, Kim HK, Kim SS, Sim DS, Hong YJ, Kim JH, Ahn Y (2017) Long-term preclinical evaluation of bioabsorbable polymer-coated drug-eluting stent in a porcine model. Macromol Res 25:730–738. https://doi.org/10.1007/s13233-017-5067-z
54. Kim JH, Ko NR, Jung BY, Kwon IK (2016) Development of a novel dual PLGA and alginate coated drug-eluting stent for enhanced blood compatibility. Macromol Res 24:931–939. https://doi.org/10.1007/s13233-016-4130-5

55. Zamani M, Prabhakaran MP, Varshosaz J, Mhaisalkar PS, Ramakrishna S (2016) Electrosprayed Montelukast/poly (lactic-*co*-glycolic acid) particle based coating: a new therapeutic approach towards the prevention of in-stent restenosis. Acta Biomater 42:316–328. https://doi.org/10.1016/j.actbio.2016.07.007
56. Tsuji H, Mizuno A, Ikada Y (2000) Properties and morphology of poly(L-lactide). III. Effects of initial crystallinity on long-term in vitro hydrolysis of high molecular weight poly(L-lactide) film in phosphate-buffered solution. J Appl Polym Sci 77:1452–1464. https://doi.org/10.1002/1097-4628(20000815)77:73.0.CO;2-S
57. Elsawy MA, Kim K-H, Park J-W, Deep A (2017) Hydrolytic degradation of polylactic acid (PLA) and its composites. Renew Sustain Energy Rev. https://doi.org/10.1016/j.rser.2017.05.143
58. De Jong SJ, Arias ER, Rijkers DTS, Van Nostrum CF, Kettenes-Van Den Bosch JJ, Hennink WE (2001) New insights into the hydrolytic degradation of poly(lactic acid): participation of the alcohol terminus. Polymer 42:2795–2802. https://doi.org/10.1016/S0032-3861(00)00646-7
59. Weir NA, Buchanan FJ, Orr JF, Farrar DF, Dickson GR (2004) Degradation of poly-L-lactide. Part 2: increased temperature accelerated degradation. Proc Inst Mech Eng H 218:321–330. https://doi.org/10.1243/0954411041932809
60. Fabra MJ, Talens P, Chiralt A (2008) Tensile properties and water vapor permeability of sodium caseinate films containing oleic acid-beeswax mixtures. J Food Eng 85:393–400. https://doi.org/10.1016/j.jfoodeng.2007.07.022
61. Rosli NA, Karamanlioglu M, Kargarzadeh H, Ahmad I (2021) Comprehensive exploration of natural degradation of poly(lactic acid) blends in various degradation media: a review. Int J Biol Macromol 187:732–741. https://doi.org/10.1016/j.ijbiomac.2021.07.196
62. Göpferich A (1996) Mechanisms of polymer degradation and erosion1. Biomater Silver Jub Compend 17:117–128. https://doi.org/10.1016/B978-008045154-1.50016-2
63. Zhou J, Wang X, Hua K, Duan C, Zhang W, Ji J, Yang X (2013) Enhanced mechanical properties and degradability of poly(butylene succinate) and poly(lactic acid) blends. Iran Polym J (English Edition) 22:267–275. https://doi.org/10.1007/s13726-013-0124-8
64. Alshomer F, Chaves C, Kalaskar DM (2018) Advances in tendon and ligament tissue engineering: materials perspective. J Mater 2018:1–17. https://doi.org/10.1155/2018/9868151
65. De Santis R, Sarracino F, Mollica F, Netti PA, Ambrosio L, Nicolais L (2004) Continuous fibre reinforced polymers as connective tissue replacement. Compos Sci Technol 64:861–871. https://doi.org/10.1016/j.compscitech.2003.09.008
66. Johnson GA, Tramaglini DM, Levine RE, Ohno K, Choi N-Y, Woo SL-Y (1994) Tensile and viscoelastic properties of human patellar tendon. J Orthopaed Res 12:796–803. https://doi.org/10.1002/jor.1100120607
67. Svensson RB, Hansen P, Hassenkam T, Haraldsson BT, Aagaard P, Kovanen V, Krogsgaard M, Kjaer M, Magnusson SP (2012) Mechanical properties of human patellar tendon at the hierarchical levels of tendon and fibril. J Appl Physiol 112:419–426. https://doi.org/10.1152/japplphysiol.01172.2011
68. Peltonen J, Cronin NJ, Avela J, Finni T (2010) In vivo mechanical response of human Achilles tendon to a single bout of hopping exercise. J Exp Biol 213:1259–1265. https://doi.org/10.1242/jeb.033514
69. Michael FM, Khalid M, Walvekar R, Ratnam CT, Ramarad S, Siddiqui H, Hoque ME (2016) Effect of nanofillers on the physico-mechanical properties of load bearing bone implants. Mater Sci Eng C 67:792–806. https://doi.org/10.1016/j.msec.2016.05.037
70. Senra MR, Vieira Marques MF (2020) Synthetic polymeric materials for bone replacement. J Compos Sci 4:1–16. https://doi.org/10.3390/jcs4040191
71. Marei NH, El-Sherbiny IM, Lotfy A, El-Badawy A, El-Badri N (2016) Mesenchymal stem cells growth and proliferation enhancement using PLA vs PCL based nanofibrous scaffolds. Int J Biol Macromol 93:9–19. https://doi.org/10.1016/j.ijbiomac.2016.08.053
72. Macías-Martínez BI, Cortés-Hernández DA, Zugasti-Cruz A, Cruz-Ortíz BR, Múzquiz-Ramos EM (2016) Heating ability and hemolysis test of magnetite nanoparticles obtained by a simple co-precipitation method. J Appl Res Technol JART 14:239–244. https://doi.org/10.1016/J.JART.2016.05.007

Authors and Affiliations

Mónica Elvira Mendoza-Duarte[1,2] · Jorge Alberto Roacho-Pérez[3] · Adriana G. Quiroz- Reyes[3] · Elsa N. Garza-Treviño[3] · Celia N. Sánchez-Domínguez[3] · Perla Elvia García-Casillas[4] · Alejandro Vega-Rios[1]

✉ Mónica Elvira Mendoza-Duarte
monica.mendoza@cimav.edu.mx

✉ Alejandro Vega-Rios
alejandro.vega@cimav.edu.mx

Jorge Alberto Roacho-Pérez
alberto.roachoprz@uanl.edu.mx

Perla Elvia García-Casillas
perla.garcia@ciqa.edu.mx

[1] Department of Engineering and Chemistry of Materials, Centro de Investigación en Materiales Avanzados, Av. Miguel de Cervantes #120, 31136 Chihuahua, Chihuahua, Mexico

[2] Institute of Engineering and Technology, Universidad Autónoma de Ciudad Juárez, Ave. Del Charro 450 Norte, 32310 Ciudad Juárez, Mexico

[3] Department of Biochemistry and Molecular Medicine, School of Medicine, Universidad Autónoma de Nuevo León, 64460 Monterrey, Mexico

[4] Advanced Materials Area, Centro de Investigación en Química Aplicada, Blvd. Enrique Reyna Hermosillo No. 140, 25294 Saltillo, Mexico